TECHNOLOGY DEVELOPMENT OF FAST-RESPONSE AERODYNAMIC PRESSURE PROBES

P. Gaetani – G. Persico

Laboratorio di Fluidodinamica delle Macchine, Dipartimento di Energia, Politecnico di Milano
Via Lambruschini 4, I-20158 Milano, Italy

paolo.gaetani@polimi.it, giacomo.persico@polimi.it

ABSTRACT

The paper presents and discusses the recent developments on the Fast-Response Aerodynamic Pressure Probe (FRAPP) technology at the Laboratorio di Fluidodinamica delle Macchine (LFM) of the Politecnico di Milano. At first the different geometries developed and tested at LFM are presented and critically discussed: the paper refers to single-sensor or two-sensor probes applied as virtual 2D or 3D probes for phase-resolved measurements. The static calibration of the sensors inserted inside the head of the probes is discussed, also taking into account for the temperature field of application: in this context a novel calibration procedure is discussed and the new manufacturing process is presented. The dynamic calibration is reconsidered in view of the 15 years experience, including the extension to probes operating at different temperature and pressure levels with respect to calibration. As for the probe aerodynamics, the calibration coefficients are discussed and the most reliable set here evidenced. A novel procedure for the quantification of the measurement uncertainty, recently developed and based on the Montecarlo methodology, is introduced and discussed in the paper.

KEYWORDS

FRAPP, PRESSURE SENSOR, TEMPERATURE CORRECTION, TRANSFER FUNCTION, AERODYNAMICS, UNCERTAINTY QUANTIFICATION,

NOMENCLATURE

c: sound speed
P: pressure
ω_n: natural frequency
ζ: non dimensional damping
μ: dynamic viscosity
ρ: density
T: temperature
U: uncertainty
KPs, Kpt: sensitivity coeff. to static and total pressure
Kyaw, Kpitch: sensitivity coeff. to the yaw, pitch angles

INTRODUCTION

Measuring the unsteady flow downstream of turbomachinery rotors passed from being a ‘niche’ research activity in the nineties to become a common practice the scientific studies of present-day turbomachinery (Roduner et al., 2000, Gaetani et al., 2010, Gaetani et al., 2012, Lengani et al., 2014, Gatti et al., 2017), with also relevant examples of industrial applications (Brouckaert 2007, Toni et al., 2010, Guidotti et al., 2011). Such evolution was sustained by the technical development of instrumentation technology, of novel data-reduction methods, and on the practical experience of the experimentalists. A key contribution to this development came from one specific measurement technology, i.e. the Fast Response Aerodynamic Pressure Probe (FRAPP), which has undoubted advantages with respect to other intrusive or non-intrusive techniques in terms of rigidity, reliability, promptness, and, last but not least, in the fact that it provides pressure measurements, which can be used for the evaluation of the blade-row and stage performance. Thanks to the very high temporal

resolution, these probes also allowed investigating experimentally complex flow phenomena connected to unsteady blade row interaction (Miller at al., 2003, Schlienger et al., 2004, Gaetani et al., 2006, Paradiso et al., 2008, Persico et al., 2009).

The FRAPP concept comes from the combination of fast-response pressure transducers, typically of piezoresistive kind, with aerodynamic directional pressure probes. The transducers can be flush-mounted on the probe head (Ainsworth et al., 1995), enhancing the frequency response despite to fragility, but in other examples (Heneka 1983, Gossweiler et. al., 1995, Kupfershmied et al., 2000, Brouckaert, 2007) the researchers preferred to embed the transducers within the probe head, to enhance the probe strength. Excellent reviews on the early stages of FRAPP development can be found in Sieverding et al., 1998, Ainsworth et al., 2000, and Kupfershmied et al., 2000. However, since then further relevant improvements were made on the basic technology and some of them are reported in the very recent review proposed by Lepikovsky, 2018.

A specific version of FRAPP technology has been object of research and development at Politecnico di Milano since 1998. The probe concept, that is alternative with respect to what proposed by the authors listed above, was first proposed by Barigozzi et al., 2000, and further elaborated by Persico et al., 2005a. With the aim of minimizing the probe blockage while maximizing the instrumentation reliability, an optimal configuration was identified by using single- or two-sensor probes operated as virtual three- of four-sensor probes, and by adopting commercial transducers that only need to be mounted and glued within the probe head. This design implies the adoption of a relatively large line-cavity system connecting the pressure tap on the probe head to the sensor, strongly influencing the probe dynamic response. However, dedicated computational studies and the set-up of a novel dynamic calibration facility (Persico et al., 2005b) has led to develop FRAPPs featuring dynamic response of the order of 100 kHz after digital compensation with the experimental transfer function.

This paper proposes a review of the most relevant advances in FRAPP technology conceived and applied at Politecnico di Milano in the last decade, in terms of high-temperature applications, dynamic identification and uncertainty quantification, analyzing systematically probes for two-dimensional and three-dimensional measurements.

FRAPP DESCRIPTION

Before discussing technological aspects and metrological issues, this section proposes a review of the current probes shape configurations and its implication on the measurement capability. Two probes are considered, one cylindrical for two-dimensional flow measurements and one hemispherical for three-dimensional flow measurements. Even though the probes share several technical features, they are discussed separately in the following.

Cylindrical probe

The cylindrical shape makes the probe inherently suitable for measuring the flow direction in a plane normal to the cylinder axis (called yaw angle in the following), alongside the total and static pressure. Conversely, it has a low sensitivity to the flow components parallel to the axis and hence to the related flow angle, called pitch in the following, so that it can be considered insensitive for pitch angles values within ±10°, as it results after a dedicated test campaign. As the probe embeds a single sensor for miniaturization, it needs three pressure readings measured at different rotations around the probe axis to virtually simulate the operation of a three-sensor probe. This prevents from performing real-time unsteady measurements; however, unless operation instabilities are of concern, in case of unsteady turbomachinery flows this is not a severe limitation as one is typically interested in the periodic component of the flow unsteadiness. The unsteady periodic component can be extracted by means of ensemble averages locked on the rotor wheel, using a key-phasor signal. The virtual operation prevents from achieving direct turbulence measurements, even if estimates of the turbulence intensity are possible considering the signal acquired by the probe at the angular position aligned to the phase-averaged flow direction, if the unresolved flow angle fluctuations are sufficiently

low (± 9°, see Persico et al., 2008).

The probe size and shape are determined by the sensor characteristics. The cylindrical shape was selected to miniaturize as much as possible the probe, thus reducing the probe blockage. The probe is, in practice, manufactured around one of the smallest transducers commercially available, which has just to be inserted within the cylinder and glued with a proper material. In this way the size of the probe can be minimized down to about 2 mm. The smooth shape of the probe, combined with its miniaturization, guarantees an optimal probe aerodynamics in terms of dynamic errors, according to dedicated studies performed at the early stages of FRAPP technology development (Humm, 1994).

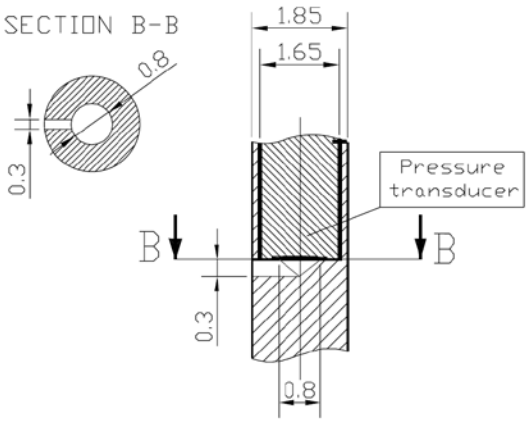

Figure 1: Representation of the cylindrical FRAPP

The probe design concept allows to deal with relatively high temperature. Present-day piezoelectric transducers can operate up to about 550 K and epoxy resins are commercially available for temperature greater than 600 K; the combination of these two elements allows manufacturing high-temperature FRAPP in a straightforward way and without external cooling - a topic that, however, was object of dedicated investigations (Mersinligil et al., 2011) that proved to be successful at the cost of an increase of probe blockage.

A further specific aspect of the present design is related to the installation of the sensor inside the probe head, and to the subsequent line-cavity system connecting the pressure tap on the probe head to the sensor. The topic is treated in detail in Persico et al., 2005a, in which several analytical and numerical techniques are used and compared to optimize the shape of internal cavities so to maximize the probe promptness. By virtue of this study, the promptness of the FRAPP resulted of the about 80 kHz. Such value resulted sufficiently high to match the specifications of all the FRAPP applications considered by the authors in the following decade.

Hemispherical probe

To overcome the limitations in measurement capability of cylindrical probes, also a FRAPP suitable for unsteady 3D measurements was developed at Politecnico di Milano.

In order to enhance the sensitivity to the flow components parallel to the probe axis, the probe head features a hemispherical shape with two pressure taps. The combination of the geometrical constraints imposed by the transducers as well as by the miniaturization of external and internal dimensions, led to a head diameter of 3.8 mm and to a diameter of 0.3 mm of the two pneumatic lines feeding the cavities facing the two sensors.

One pressure tap is drilled on the probe tip, with an inclination of 60° with respect to the probe axis, and it is employed only for measurement of the pitch angle. The other pressure tap is drilled on the equatorial plane, with an inclination of 90° with respect to the probe axis: it can be aligned to the ‘pitch’ tap as shown in Figure 2 or it can be rotated with respect to that by 180° around the probe stem.

The probe operating mechanism is still based on multiple pressure readings taken at different rotations of the probe around its own stem: the combined use of four pressure readings allows measuring both the flow directions, alongside total and static pressure. The configuration shown in Figure 2 allows to

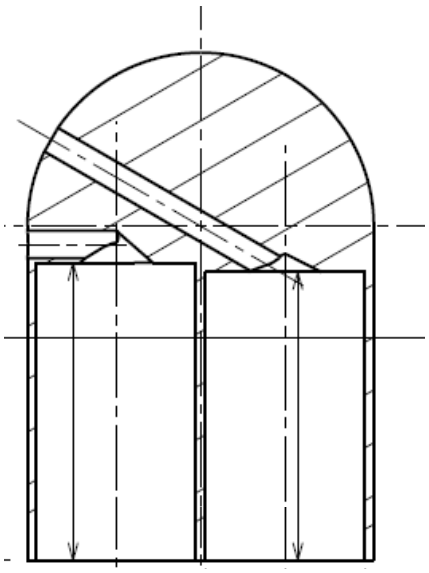

Figure 2: Representation of the hemispherical FRAPP with aligned taps

reconstruct both the flow directions with just 3 rotations, while 4 rotations are required for the configuration with 2 opposed taps (a further rotation shifted by 180° with respect to the central one of the others); however, the use of opposed taps allows reducing the dimension of the internal cavities, as in this latter case a shorter line connects the 'pitch' tap to the sensor. Theoretical estimates and experimental dynamic calibrations showed a reduction of promptness to 40 kHz, about the half of the one of the hemispherical FRAPP with opposite taps, but still very high for typical turbomachinery applications.

THERMALLY-CORRECTED CALIBRATION OF THE PRESSURE SENSOR

Due to the sensor sensitivity to the temperature, a sensor calibration in pressure and temperature is required, before performing the aerodynamic and the dynamic ones. The sensor sensitivity to temperature is measured by applying an additional resistance ("sense resistor" in the following) on the bridge as showed in figure 3. The voltage drop across the sense resistor (ΔV_T) is mainly function of the current flowing across the bridge, which depends on the bridge temperature. Thus, by reading the voltage difference across the bridge (ΔV_P) and ΔV_T, the sensor behavior can be fully documented.

The probe temperature is set by inserting it in an oven: the insertion length is chosen to be representative of what needed in the real application, so to minimize the effect of the thermal conduction along the stem.

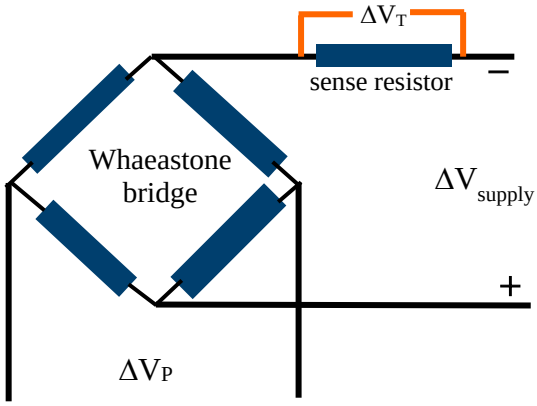

Figure 3: electrical scheme for the pressure and temperature calibration

The calibration procedure applies as follow: first the oven temperature is set and a consistent waiting time (typically 30 minutes) is scheduled to bring the probe in a steady thermal condition. Then a pressure ramp is applied up to the calibration range foreseen for the tests. To include possible hysteretic behavior in the calibration coefficients and uncertainty, the pressure ramp has both positive and negative slopes. Then, the oven temperature is modified and the procedure repeated: also for the temperature ramp, positive and negative slopes can be applied.

For each temperature level (T_i), the pressure data are then fit by linear function: the results are the slope (K_{Pi}), intercept (Q_{Pi}) and uncertainty (U_{Pi}).

K_{Pi}, Q_{Pi}, U_{Pi}, are then fit by polynomial functions (typically linear or parabolic, depending on the trend), to have the K_P and Q_P (as function of the ΔV_T). The sensor temperature T_i and ΔV_{Ti} can also be fitted to have K_T , Q_T. Figure 4 shows typical calibration results.

The procedure is accurate and its only critical point is a random offset on Q_{Ti} due to the sensor thermal sensitivity, while the K_{Ti} is perfectly repeatable: this occurrence, whose magnitude unfortunately depends on the single transducer, requires an online check to measure it during tests.

Once K_T , Q_T and K_P , Q_P are found, during the probe application the sensor Pressure and temperature can be calculated by:

$$P = K_P \times \Delta V_P + Q_P \qquad (1); \qquad T = K_T \times \Delta V_T + Q_T \qquad (2);$$

Uncertainty quantification

The uncertainty evaluation is made by considering the uncertainty on each measured point in pressure for a given oven (probe) temperature and the contribution due to the least square interpolation among the pairs (P_i, ΔV_{Pi}). The contribution on the single measured point takes into account the standard deviation of the population, the reference transducer uncertainty, the data acquisition board analog-digital converter specifications: Gaussian distribution have been considered for the first two quantities while a rectangular distribution have been applied to the AD converter. All these contributions are considered not cross correlated, are made homogeneous in terms of units and

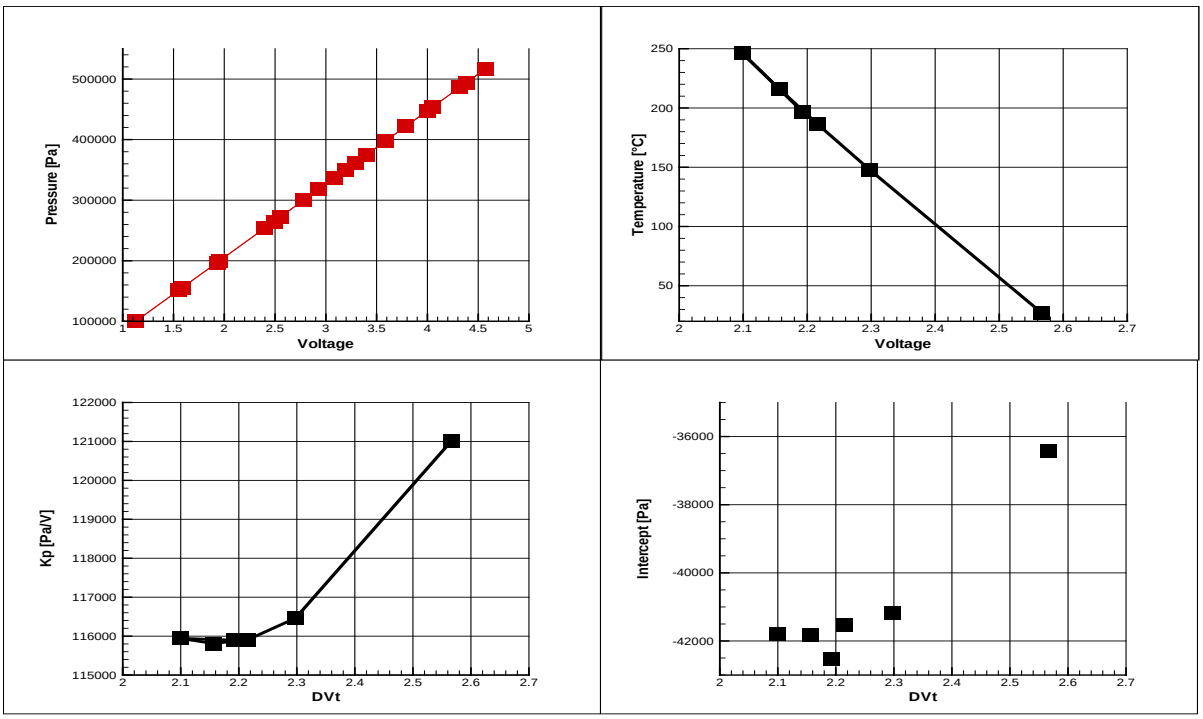

Figure 4: calibration coefficients:
a) pressure- voltage at a given temperature T_i; b) sensor temperature vs ΔV_T
b) sensor temperature vs ΔV_T; d) sensor temperature vs ΔV_T

are considered to include 95% of the Gaussian distribution data: finally, given the functional dependence $f = f(x_1, x_2, \ldots, x_n)$, the uncertainty propagation approach is considered:

$$U = \sqrt{\sum_{i=1}^{n} \left(u_i \frac{\partial f}{\partial x_i}\right)^2}. \quad (3);$$

To couple the uncertainty on the single calibration point and the one due to the least square interpolation, the highest among the single points one is considered. Overall for a 6 bar_a transducer, the following results are found (fig. 5): no clear trends are visible and data less than 0.1% of the full range. These results are then applied during the aerodynamic calibration to get an estimation of the flow field detection uncertainty.

With the aim of comparing classical uncertainty analysis with an alternative systematic approach, the Montecarlo methodology was also applied and the same contributions to the uncertainty were considered. The data for each temperature level (T_i) were interpolated by a least square method by introducing N (a number high enough to get a statistical reliability) different pairs (P, V_P) chosen randomly into the populations characterized by the selected distributions. The results of the N calculations were N line constants and intercepts, statistically treated to get mean values (K_{Pi}, Q_{Pi}) and their standard deviations. As a following step, the M pairs of data belonging to the population (K_{Pi}, ΔV_{Ti}) were randomly chosen according to a Gaussian distribution, then averaged to get $Kp = Kp(\Delta V_T)$ and its standard deviation; the same methodology was applied to the intercept. In this way $P = P(\Delta V_T)$, and its standard deviation were available for the application in the aerodynamic calibration. To get a proper accuracy, the Montecarlo procedure requires a huge number of iteration: to make the procedure

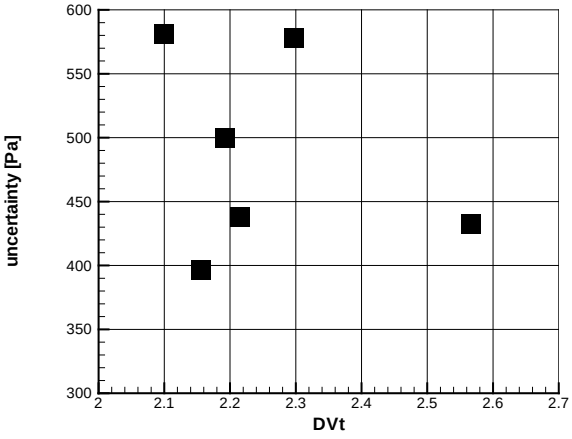

Figure 5: extended uncertainty for the different probe temperature

affordable the Latin hypercube methodology was applied to support pairs choice, and a convergence criterion was also set on the standard deviation value. Results got by the two methodologies showed a good consistency and were the basis for the determination of the uncertainty in the aerodynamic calibration. Figure 6 shows results of the uncertainty calculation when reported on the same chart of the probe pressure for a Mach=0.5 test: the average uncertainty covering 95% of the samples is about 5 mbar, that is the same order of magnitude of the previous methodology.

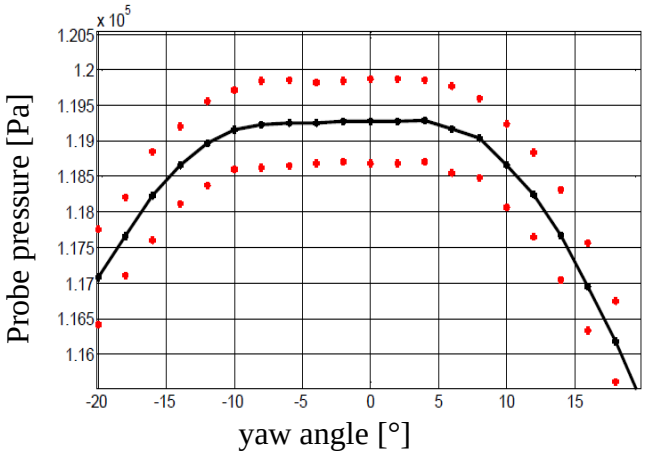

Figure 6: uncertainty range for a test at Mach equal to 0.5

FRAPP DYNAMIC ANALYSIS

The manufacturing concept of the FRAPP developed at PoliMi implies a promptness reduction due to the line-cavity system between the pressure tap and the sensor. However, a proper design of the internal cavities allows obtaining a promptness of 80 kHz, as shown in Persico et al., 2005a.

To reach such promptness the probe transfer function has to be experimentally determined and then applied in the data processing of measurements in test-rigs. However, some difficulties arise since dedicated dynamic calibration facilities are not widespread and the interpretation of results is not straightforward, due to the potential presence of non-linear effects as well as measurement uncertainties that inevitably affect also dynamic calibration tests. Moreover, the use of the transfer function for experiments downstream of turbomachinery rotors poses further problems as the operative conditions are different between calibration and tests, as discussed in the following.

Time- and frequency-domain identification

The dynamic calibration of fast-response pressure instrumentation poses, at first, technical issues related to the generation of input signals featuring unsteady perturbations at sufficiently high frequency. Siren disks (Sahin, 2018) are used if periodic stimulus signals are of interests, while shock tubes (Persico et al., 2005b, Brouckaert 2007) are selected if a transient non-periodic signal is of concern, as the bursting of a diaphragm generates a travelling shock wave that acts as step signal.

Shock tubes are convenient as, in a single test, the dynamic response of the probe can be achieved for the full frequency range typically of interest for turbomachinery applications (100 kHz). Considering air at ambient conditions, the dynamic content of a traveling shock involves frequencies up to the order of MHz. By setting proper diaphragm features, shock amplitude can be selected in the range of typical pressure fluctuations in turbomachinery (in the order of tenths of bars or even less as authors documented in Gaetani et al., 2007, Paradiso et al., 2008, Toni et al., 2010, Guidotti et al., 2011); such perturbations are normally small enough to not activate relevant non-linear effects in the dynamic evolution of the pressure field within the line-cavity system. By virtue of such physical linearization, the transfer function determined through a step-response is applicable for the measurement of the periodic fluctuations occurring within turbomachinery.

A dedicated development is continuously ongoing at Politecnico di Milano on the low-pressure shock tube developed for dynamic calibration, since its first presentation in Persico et al., 2005b. Most of the development is focused on the improvement of the diaphragm, searching for materials that feature a fast and as complete as possible burst, and generating a shock as weak as possible.

By present-day plastic diaphragms, shock strengths of the order of 0.2-0.3 bars are obtained. They exhibit incomplete opening whose effects were investigated in detail in Gaetani et al., 2008, and can be properly handled without affecting in a relevant way the determination of the transfer function. Figure 7a presents a typical experimental transfer function obtained with the method proposed in Persico et al., 2005a. The experimental trend recalls closely the one of a second-order linear system,

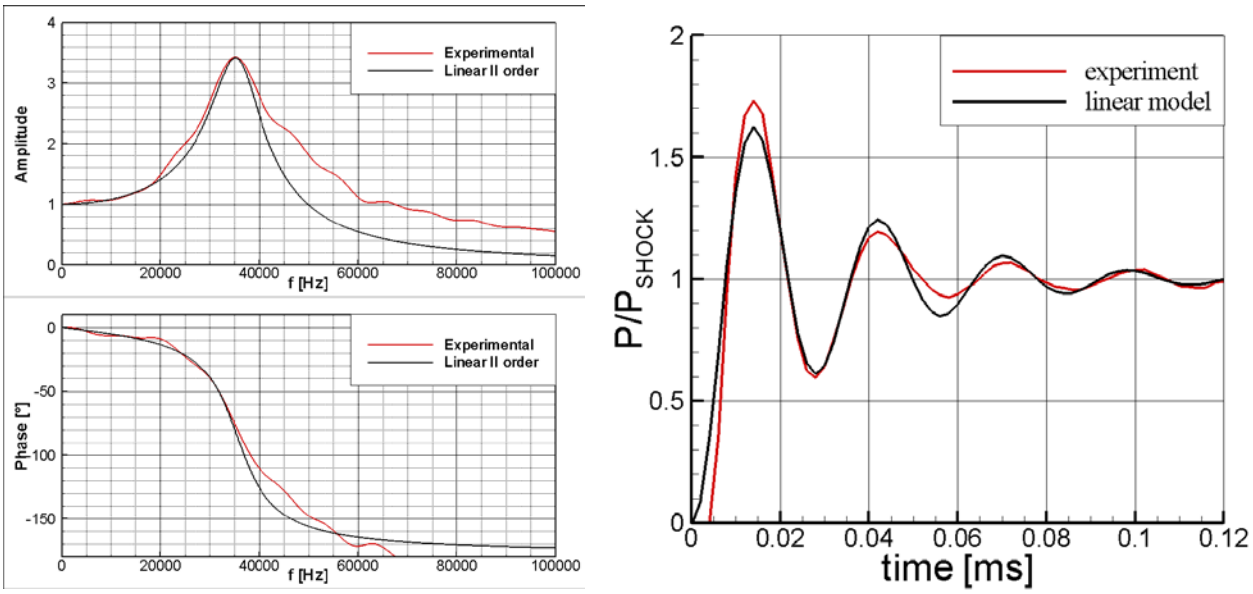

(a) (b)

Figure7: Frequency-domain (a) and time-domain (b) identification of a typical FRAPP

with an evident peak at about 35 kHz representing the probe resonance. On the basis of the values of frequency and amplitude at the resonance, the system identification can be done: the corresponding linear system is also plotted in comparison to the experimental one. Differences exist but occur at high frequency (above 40 kHz). To provide a more intuitive idea of the observed non-linearity, the measured step response and the analytical one are plotted in Figure 7b. The experimental trend reproduces well the one of the analytical model, suggesting that the modeling is reliable for the whole response. The highest difference is concentrated in the first overshoot, in which the experiment exhibits a steeper pressure rise and a higher peak. The faster pressure rise at the beginning of the process is clearly responsible for the non-linearity observed in the frequency domain beyond 40 kHz. Since full linearity is not guaranteed a-priori, experimental dynamic calibration proves to be crucial to characterize the FRAPP transfer function and its application to measured signals.

Pressure and temperature correction

The high degree of linearity exhibited by the FRAPP allows the use of the transfer function to dynamically compensate the pressure signals measured in turbomachinery test rigs. However, the fluid thermodynamic conditions are often different from those occurring in the shock tube, and in general it is not possible to reproduce in the shock tube facility the high-pressure and high-temperature levels of the turbomachinery experiment.

However, relatively simple techniques can be proposed for correcting the transfer function identified in the dynamic calibration experiments. In Persico et al., 2005a, the analytical model of Hougen et al., 1963 was found to reproduce fairly well the resonance frequency of the FRAPP. This model, as well as others available in literature, shows that, apart from geometrical terms, the natural frequency and the non-dimensional damping of the line-cavity system exhibit the following dependencies:

$$\omega_N \propto c \propto \sqrt{T} \qquad (4)$$

$$\zeta \propto \frac{\mu}{c\rho} \propto \mu(T)\frac{\sqrt{T}}{P} \qquad (5)$$

Expressions 4, which relates directly the natural frequency to the sound speed, is intuitively justified as the dynamic response of the line-cavity system depends on the pressure waves propagation within the probe internal cavities. In the context of perfect gases, this property provides a first straightforward correction to the transfer function for temperature differences between calibration and application. Expression 5 indicates that both temperature and pressure levels have an impact on the damping and, once again, it provides a tool for correcting the transfer function identified with

experiments in the shock tube; also the pressure level can have an effect and demands for corrections, even though quantitatively minor with respect to that of the temperature.

Figure 8 shows the impact of combined temperature and pressure correction on the amplitude of the transfer function determined in the shock tube. For this probe, a nearly perfect dynamic linearity is observed up to 60 kHz, with natural frequency at about 40 kHz. By considering an application at the maximum temperature level technically available for the FRAPP (550 K) the correction was applied to the analytical transfer function. The impact of the corrections remains limited up to 20 kHz, while a relevant deviation occurs for frequency higher than 40 kHz. The test rig application, not reported for confidentiality reasons, showed that the correction allowed obtaining more realistic picture of the high-frequency oscillations occurring in real turbomachines.

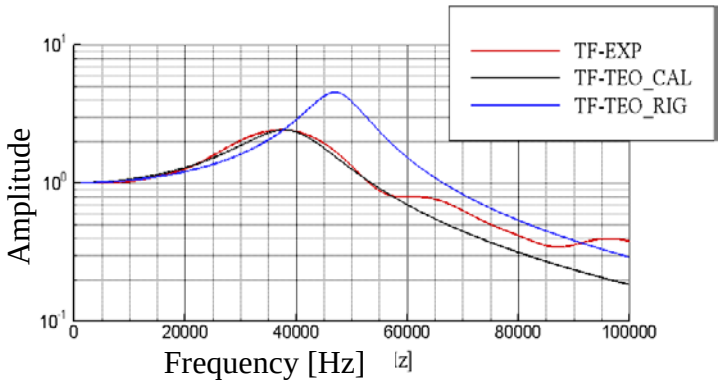

Figure 8: Impact of temperature of tests with respect to calibration on FRAPP transfer function

FRAPP AERODYNAMICS

The aerodynamic calibration is performed on a convergent nozzle, whose outlet section is 50 mm x 60 mm and, for standard probes, it typically allows for neglecting the blockage effects up to Mach = 0.95. Convergent – divergent nozzles are also available when supersonic calibrations are required. The Reynolds – Mach number effects decoupling can be also achieved by a nozzle inserted in a duct brought to a chocked condition by a downstream throat. The outlet pressure is usually set to be atmospheric and the Mach number is set by imposing the total pressure in the upstream reservoir.

When the aerodynamic calibration is of concern, different calibration coefficients can be taken into account. The advantages of different coefficient sets may arise from a pure aerodynamic behaviour or from the uncertainty point of view.

Cylindrical FRAPP

For the 2D Frapp probe, it is commonly applied the following:

$$Kyaw = \frac{P_L - P_R}{P_T - P_S} \qquad KP_T = \frac{P_T - P_C}{P_T - P_S} \qquad KP_S = \frac{P_S - (P_R + P_L)/2}{P_T - P_S}$$

where: P_L = probe Left pressure reading, P_R = probe Right pressure reading, P_C = probe Central pressure reading, P_T = nozzle Total pressure, P_S = nozzle Static pressure.

The experimental trends of the coefficients are reported in Figure 9: when the Kyaw coefficient is zero, the aerodynamic reference direction is set. The range of monotonic trend is typically up to +/- 23°, due to the 45° degrees of spacing between the 3 pressure readings (Left, Central, Right) and to the range in between the two separation points of the cylinder flow in cross flow, that is around +/-

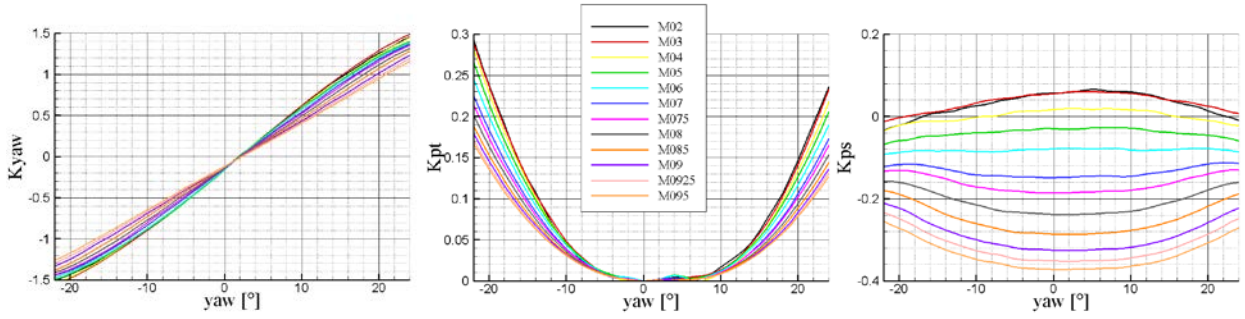

Figure 9: 2D FRAPP calibration coefficients for varying Mach number and yaw angle.

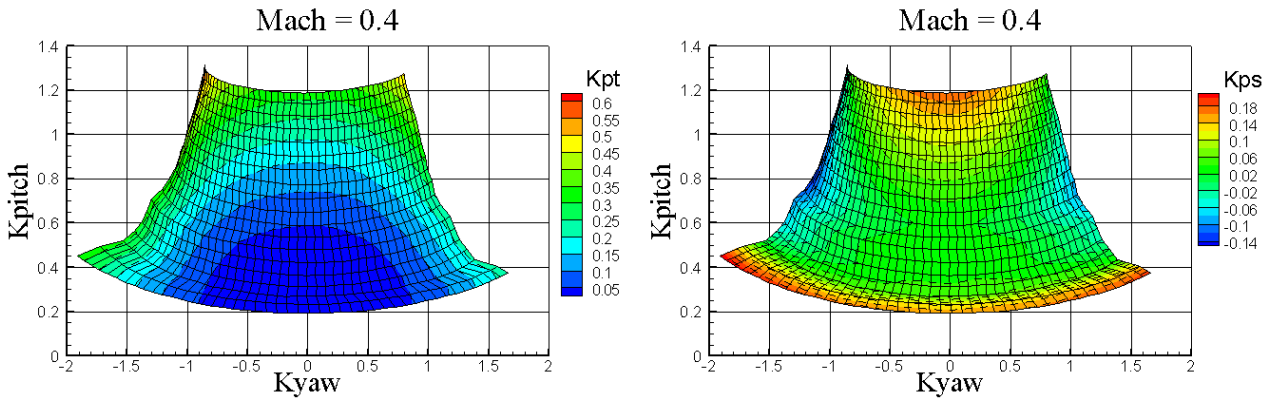

Figure 10: Kpt and Kps on the Kyaw and Kpitch coefficient grid for 3D FRAPP (range ± 22°)

67 ÷ 70 deg. depending on the probe, Reynolds and Mach number. The total pressure coefficient differs for the compressibility effects over the probe cylindrical head.

In the application phase, the real Total and Static pressures (and by these the Mach number) and the flow angle are derived by an iterative procedure. First the static pressure and the total pressure are chosen as the average between the left and right, and the central one, respectively; by these the Kyaw is a calculated and the yaw angle is derived. By the yaw angle, the new KPt and KPs are calculated making use of the calibration curves, properly interpolated in angles and Mach. At this point, the new Total and Static pressures are calculated and the second iteration can start.

In case of thermal drift, the Kyaw is less sensitive than KPt and KPs because the numerator is almost insensitive to the drift, which typically occurs in the form of an offset.

Hemispherical FRAPP

For the 3D hemispherical FRAPP several sets of coefficients were considered and evaluated in calibration. They are discussed separately in the following.

- **set A:**

$$Kyaw = \frac{P_L - P_R}{P_T - P_S} \qquad Kpitch = \frac{P_T - P_P}{P_T - P_S} \qquad KP_T = \frac{P_T - P_C}{P_T - P_S} \qquad KP_S = \frac{P_S - (P_R + P_L)/2}{P_T - P_S}$$

where Kyaw, KP_T and KP_S depend on the yaw taps (and its virtual readings) and on the flow total and static pressures, while the Kpitch depends on the Pitch tap (P_P) and on the flow total and static pressures. None of the coefficients is defined by mixing the pitch and the yaw tap and all include P_T and P_s. As reported in Figure 10, the Kpt and Kps coefficients are regular over the grid Kyaw-Kpitch and for this easily applicable. The drawback is the overlapping at the Kyaw borders that brings to a non unique solution during the interpolation procedure.

- **set B:**

It differs from Set A only for: $Kyaw = \frac{P_L - P_R}{P_{max} - (P_L + P_R)/2}$ where P_{max} is the maximum value of the parabola passing by the 3 points P_C, P_L, P_R: it is an artificial value because the pressure curve around a cylinder is not a parabola although similar to that. This new coefficient does not suffer from an offset being only related to one transducer and including differences both at numerator and denominator. A similar choice for the *Kpitch* cannot be applied because there are no virtual taps for such quantity as result of the rotation along the probe

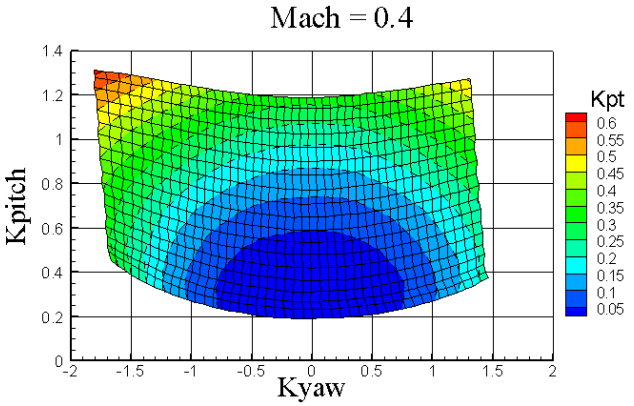

Figure 11: Kpt on the Kyaw and Kpitch coefficient grid (range +/- 22°)

stem. The other main advantage concerns the grid regularity that allows for a proficient interpolation all over the angular range, as visible in Figure 11.

- **set C:**

It differs from the Set A only by the *Kpitch* that is defined in this set as: $itch = \frac{P_C - P_P}{P_T - P_S}$.

This choice allows for a direct link between the central reading of the yaw and the pitch tap, being the central reading for the yaw in any case dependent on the pitch flow angle. This set, even though seeming smart, in fact connects the two sensors readings and, in case of drift, it may increase substantially the final uncertainty. From the purely aerodynamic point of view, as shown in Figure 12, it changes the Kpitch coefficient magnitude but does not fix the overlapping at the grid boundary.

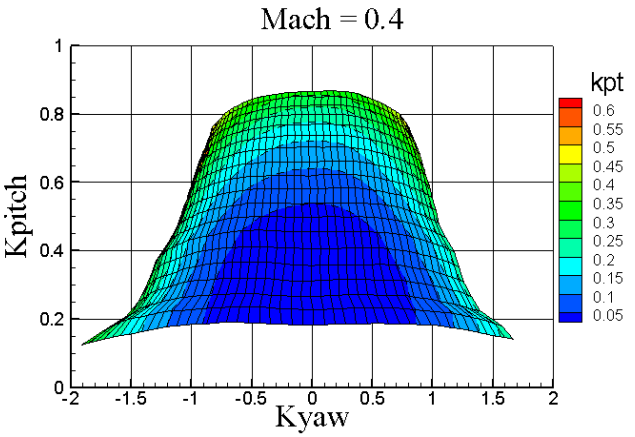

Figure 12: Kpt on the Kyaw and Kpitch coefficient grid (range +/- 22°)

Uncertainty Quantification

To quantify the uncertainty level in the calibration matrixes building and application, the same methodologies described in the static calibration can be applied. As the calibration matrixes require the application of iterative procedures, the Montecarlo methodology is particularly attractive for computing the uncertainty propagation.

The calibration coefficients (Kyaw, Kpitch, Kpt, Kps) were first calculated by choosing pressure values (P_L, P_C, P_R, P_P, P_T, P_S) randomly in each population (for a given Mach number and angular position) according to the Gaussian distribution resulting from the static calibration. Then, results were averaged and their standard deviation calculated, all them stored in proper calibration files.

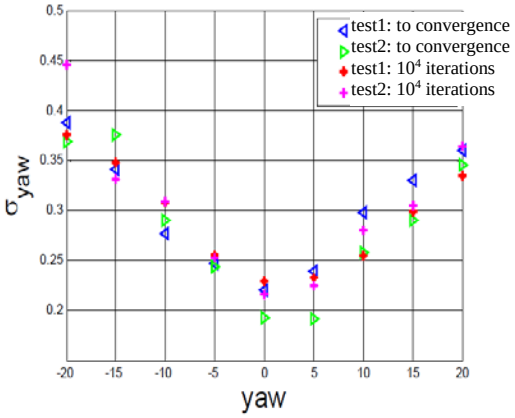

Figure 13: results in terms of standard deviation for different runs

During the measurements campaign, to get the flow quantities the measured pressures were used coupled to the calibration matrixes. A number N of different sets of pressures and coefficients were selected randomly in each population and, by an iterative procedure, the flow quantities calculated. Being the process statistical, all the data were then averaged and the standard deviation calculated. As for the result distribution, being the input data chosen according to a Gaussian distribution, the output one was of the same kind. The number N of different sets was dynamically chosen according to the convergence criterion chosen for the standard deviation change ($\Delta\sigma_{i+1,i}/\sigma_i < 10^{-3}$). Also in this case, the set choice was done by applying the Latin hypercube methodology in order to save computational time. Figure 13 shows the results for different run and convergence criteria: since the method is statistical, different runs may lead to different results.

Mach	δYaw	δM	δPt %	δPs %
0.25	0.63	0.002	1.10	1.50
0.35	0.50	0.004	0.92	2.90
0.45	0.62	0.001	0.56	0.76
0.55	0.69	0.001	0.28	0.40
0.65	0.62	0.003	0.26	0.70
0.75	0.58	0.011	0.40	0.72
0.825	0.50	0.016	0.24	1.81
0.875	0.37	0.013	0.21	2.23
0.925	0.16	0.023	0.21	2.10

Table 1: averaged errors for the Yaw, Mach, total and static pressure

Notwithstanding such possible variations, the difference is almost negligible, for a given yaw angle. Finally, Table 1 shows the averaged error for the 4 quantities of interest (yaw, Mach, Pt, Ps). Values are high typically at low and high Mach numbers. At low Mach number this is due to the high transducer range, at high Mach the overspeed on the cylinder makes the flow locally supersonic.

CONCLUSIONS

This paper has presented the most relevant developments in FRAPP technology at Politecnico di Milano in last decade. The study has considered the two most relevant probe configurations manufactured, calibrated and applied by the authors in their experience, for both 2D and 3D unsteady flow measurements in turbomachinery. Specific challenges emerged in terms of extension to (relatively) high temperature applications, simplicity of operation, improved aerodynamics and more refined uncertainty quantification, and have been all acknowledged in the paper.

In particular, uncooled FRAPPs were manufactured for temperature operation of about 550 K, without changing the external/internal probe shape and size. The need for high temperature extension has also triggered specific theoretical models to handle temperature-corrected static and dynamic calibration of the probes. Physical analysis of the sensor properties and of the line-cavity system provided general rules for correcting the static and dynamic pressure measurements performed during calibrations. In the frame of these activities, the static and dynamic calibration procedures were re-analyzed to investigate the global reliability of the FRAPP technology.

The probe aerodynamics were also reconsidered and several sets of aerodynamic coefficients have been proposed for the hemispherical FRAPP, which is less consolidated with respect to the cylindrical one. This analysis has highlighted that clear advantages can be obtained if a specific set of coefficients is applied. Finally, a novel technique based on the Montecarlo approach has been introduced to evaluate the uncertainty of FRAPP measurements, combining the one of the sensor (based on a Montecarlo analysis of the static calibration) with the formulation of the aerodynamic coefficients.

REFERENCES

Ainsworth, R. W., Allen, J. L., Batt, J J M., (1995) *The development of fast response aerodynamic probes for flow measurements in turbomachinery*. Journal of Turbomachinery, Vol 117.

Ainsworth R. W., Miller, R. J., Moss, R. W., Thorpe, S. J., (2000). *Unsteady pressure measurements.* Measurement Science and Technology, Vol. 11, pp. 1055–1076.

Barigozzi, G., Dossena, V., Gaetani, P., (2000). *Development and first application of a single hole fast response pressure probe*. Proc. 7th Symp. Measuring Techniques in Transonic and Supersonic Flow in Cascade and Turbomachines, Florence, Italy.

Brouckaert, J.F. (2007). *Fast response aerodynamic probes for measurements in turbomachines.* Proceedings of The Institution of Mechanical Engineers Part A - Journal of Power and Energy, Vol. 221, pp. 811-813.

Gaetani, P., Persico, G., Dossena, V., Osnaghi, C., (2007). *Investigation of the Flow Field in a High-Pressure Turbine Stage for Two Stator-Rotor Axial Gaps-Part II: Unsteady Flow Field*. Journal of Turbomachinery, Vol. 129, pp. 580-590.

Gaetani, P., Guardone, A., Persico, G., (2008), *Shock tube flows past partially opened diaphragms,* Journal of Fluid Mechanics, Volume 602, pp. 267-286.

Gaetani P., Persico, G., Osnaghi, C., (2010). *Effects of Axial Gap on the Vane-Rotor Interaction in a Low Aspect Ratio Turbine Stage,* Journal of Propulsion and Power, Vol. 26, pp. 325-334.

Gaetani, P., Persico, G., Mora, A., Dossena, V., Osnaghi, C., (2012). *Impeller Vaned Diffuser Interaction in a Centrifugal Compressor at Off-Design Conditions*. Journal of Turbomachinery, Vol. 134, 061034.

Gatti, G., Gaetani P., Paradiso, B., Dossena, V., Bellucci, J., Arcangeli, L., (2017), *An experimental study of the aerodynamic forcing function in a 1.5 steam turbine stage,* Journal of Engineering for Gas Turbines and Power, Vol. 139, 052503.

Gossweiler, C., Kupferschmied, P., Gyamarthy, G., (1995). *On fast-response probes, part 1: technology, calibration and application to turbomachinery*. Journal of Turbomachinery. Vol. 117

Guidotti, E., Tapinassi, L., Toni, L., Bianchi, L. Gaetani, P. , Persico, G. , (2011). *Experimental and Numerical Analysis of the Flow Field in the Impeller of a Centrifugal Compressor Stage at Design Point*. ASME paper GT2011-45036, ASME Turbo Expo 2011, Vancouver, BC, Canada.

Heneka. A., (1983) *Instantaneous three-dimensional flow measurements with a four-hole wedge probe*. Proc. of the 7th Symposium on Measuring Techniques in Turbomachines.

Hougen, J. O., Martin, O. R., Walsh, R. A., (1963) *Dynamics of pneumatic transmission lines*. Control Engineering, Vol. 10, pp. 114–117.

Humm, H. J., Gizzi, W., Gyarmathy, G., (1994). *Dynamic response of aerodynamic probes in fluctuating 3D flows*. Proc. 12th Symp. Measuring Techniques in Transonic and Supersonic Flow in Cascade and Turbomachines (Prague, Czech Republic).

Kupferschmied, P., Koppel, P., Roduner, C., Gyarmathy G., (2000). *On the development and application of the FRAP® (fast response aerodynamic probe) system for turbomachines - Part I: The measurement system*. ASME Journal of Turbomachinery, Vol. 122, Issue 3.

Kupferschmied, P., Koppel, P., Gizzi, W., Roduner, C., Gyarmathy, G., (2000). *Time-resolved flow measurements with a fast-response aerodynamic probes in turbomachines*. Measurement Science and Technology, Vol. 11, pp. 1036–1054.

Lengani, D., Paradiso, B., Marn, A., Goettlich, E., (2012). *Identification of spinning mode in the unsteady flow field of a low pressure turbine*. Journal of turbomachinery. Vol 134, 051032.

Lepicovsky, J., Simurda, D., (2018). *Past developments and current advancements in unsteady pressure measurements in turbomachines*. In press in the Journal of Turbomachinery.

Mersinligil, M., Brouckaert, J.F., Desset, J., (2011) *Unsteady Pressure Measurements With a Fast Response Cooled Probe in High Temperature Gas Turbine Environments.* Journal of Engineering for Gas Turbines and Power, Vol. 133, 081603.

Miller, R. J., Moss, R. W., Ainsworth, R. W., Horwood, C. K., (2003). *Time-resolved vane–rotor interaction in a high-pressure turbine stage*. Journal of Turbomachinery, Vol. 125, pp 1–13.

Paradiso, B., Persico, G., Gaetani, P., Schennach, O., Pecnik, R., Woisetschlger, J., (2008). *Blade row interaction in a one and a half stage transonic turbine focusing on three dimensional effects: Part I - stator-rotor interaction*. ASME paper GT2008-50291, Proc. of ASME Turbo Expo 2008: Power for Land, Sea and Air, June 9-13, 2008, Berlin, Germany.

Persico, G., Gaetani, P., Guardone A., (2005a). *Design and analysis of new concept fast-response pressure probes*. Measurement Science and Technology, Vol. 16, pp. 1741-1750.

Persico, G., Gaetani, P., Guardone A., (2005b), *Dynamic calibration of fast-response probes in a low pressure shock tube,* Measurement Science and Technology, Vol. 16, pp. 1751-1759.

Persico, G., Gaetani, P., Paradiso, B., (2008). *Estimation of turbulence by single-sensor pressure probes,* XIX Biannual Symposium on Measuring Techniques in Turbomachinery Transonic and Supersonic Flow in Cascades and Turbomachines, April 7-8, 2008, Rhode-St-Gense, Belgium.

Persico, G., Gaetani, P., Osnaghi, C., (2009). *A Parametric Study of the Blade Row Interaction in a High Pressure Turbine Stage*", Journal of Turbomachinery, Vol. 131, 031006

Roduner, C. , Kupferschmied, P. , Köppel, P., Gyarmathy, G. , (2000). *On the Development and Application of the Fast-Response Aerodynamic Probe System in Turbomachines—Part 2: Flow, Surge, and Stall in a Centrifugal Compressor*. Journal of Turbomachinery. Vol. 122, pp. 517-526.

Şahin, F.C., Schiffmann, J., (2018). *Dynamic pressure probe response tests for robust measurements in periodic flows close to probe resonating frequency*. Measurement Science and Technology, Vol. 29.

Schlienger, J., Kalfas, A. I., Abhari, R. S., (2005). *Vortex–wake– blade interaction in a shrouded axial turbine*. Journal of Turbomachinery, Vol. 127.

Sieverding, C. H., Arts, T., Denos, R., Brouckaert, J.F., (2000). *Measurement techniques for unsteady flows in turbomachines*. Experiments in Fluids, Vol. 28, pp: 285–321.

Toni, L., Ballarini, V., Cioncolini, S., Gaetani, P., Persico, G., *(2010). Unsteady Flow Field Measurements in an Industrial Centrifugal Compressor.* Proceedings of the 39th Turbomachinery Symposium, October 4-7, 2010, Houston, Texas